Direct Observation of Charge Transfer at a MgO(111) Surface

A. Subramanian,[1,*] L. D. Marks,[1] O. Warschkow,[2] and D. E. Ellis[2]

[1]*Department of Materials Science and Engineering, Northwestern University, Evanston, Illinois 60208-3108, USA*
[2]*Department of Physics and Astronomy, Northwestern University, Evanston, Illinois 60208-3108, USA*

(Received 25 June 2003; published 13 January 2004)

Transmission electron diffraction (TED) combined with direct methods have been used to study the $\sqrt{3} \times \sqrt{3}R30°$ reconstruction on the polar (111) surface of MgO and refine the valence charge distribution. The surface is nonstoichiometric and is terminated by a single magnesium atom. A charge-compensating electron hole is localized in the next oxygen layer and there is a nominal charge transfer from the oxygen atoms to the top magnesium atom. The partial charges that we obtain for the surface atoms are in reasonable agreement with empirical bond-valence estimations.

DOI: 10.1103/PhysRevLett.92.026101 PACS numbers: 68.35.Bs, 61.14.Lj, 68.37.Lp

MgO is the typical rocksalt oxide that is commonly used as a model system for testing calculations on ionic oxides. Though most studies thus far on MgO have focused on the nonpolar (001) surface, the polar (111) surface has attracted attention in recent years [1]. Experimental studies on this surface have identified various reconstructions that are remarkably stable. Critical to understanding the properties of the surface is knowledge of the electronic charge distribution. It is well established that at low angles transmission electron diffraction (TED) is highly sensitive to the distribution of bonding electrons in solids [2]. Studies of bonding charge, employing TED [3,4], thus far have been limited to bulk materials with known structures and usually involve accurate measurement (0.1%) of bulk structure factors. In contrast, the periodicities observed on reconstructed surfaces are much larger, and with proper care surface diffraction data can be treated within the kinematical approximation. Even though the accuracies obtainable for surface diffraction are poorer (1%–10%), in principle it is possible to obtain quantitative information about charge transfer between the various surface species.

In this Letter, we report the first direct measurement of charge transfer at a reconstructed surface. TEM samples of single crystal MgO (>99.95% pure and Ca <40 ppm) made from 3 mm disks were dimpled, polished, and ion beam thinned with a 5 keV Ar^+ beam to electron transparency. These were subsequently annealed in a tube furnace at 950 °C for 1.5 h in a flowing oxygen atmosphere to anneal out ion-beam damage and obtain the MgO(111)-$\sqrt{3} \times \sqrt{3}R30°$ reconstruction. After annealing, the surface exhibits extended faceting with step bunches and 200 nm wide terraces, with minimal bulk defects. TED patterns using a limited illuminated region (not selected area mode) with varying exposure times were recorded from the surface under off-zone axis conditions to minimize dynamical effects. Electron energy loss spectroscopic measurements indicated that the thickness was about 25 nm. An exposure series of ten negatives was subsequently digitized to eight bits using an optronics negative scanner calibrated to be linear, and the intensities of 266 surface reflections were measured, from 1586 raw measurements. After weighted symmetry averaging, this results in 78, 45, and 45 independent reflections for $p3$, $p31m$, and $p3m1$ plane groups, respectively. Direct methods were used to solve the structure in all three plane groups. Direct methods are a set of routines that employ *a priori* information in the form of self-consistent equations and statistical relationships between the phases of the diffracted beams. A detailed review of the techniques employed has been published elsewhere [5] and will not be discussed here. All three plane groups yielded similar solutions, and the scattering potential corresponding to the best solution is shown in Fig. 1(a). These maps with atoms assigned to the regions of sharp potential peaks were used as starting points for the refinements discussed later.

The structure that we find, shown in Fig. 1(b), is magnesium terminated with two Mg vacancies in the first layer relative to a simple bulk terminated surface. The reconstruction can be thought of as being comprised of

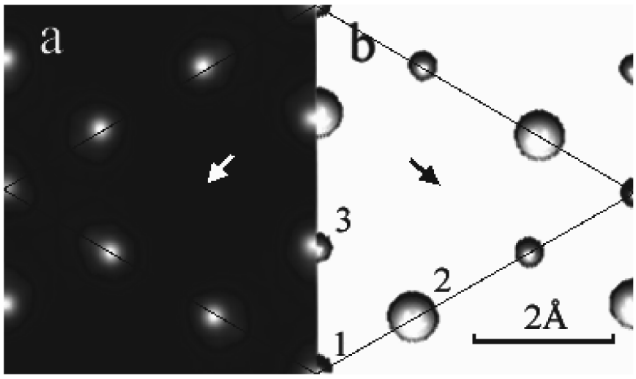

FIG. 1. (a) Direct method map for MgO(111)-$\sqrt{3} \times \sqrt{3}R30°$ surface (b) Top view schematic diagram of the same surface. Large circles correspond to O atoms and the smaller ones are Mg atoms. The numbers by each atom correspond to the layer (see Table III) and the Mg vacancies are arrowed.

complete $(MgO)_4$ octopolar units [6] with two additional O atoms in the fourth layer. The surface is therefore oxygen rich, which is consistent with previous studies [7]. We note that this structure is different from the previous model proposed for this surface by Plass *et al.* [8]; however, it should be noted that the annealing conditions we used are very different so our results do not disprove the earlier work.

Going beyond simply finding the atomic sites, we refined both the partial atomic charges of the various atoms in the reconstruction as well as their positions. Following Dawson [9] and Stewart [10], the (x-ray) atomic scattering factors were parametrized as

$$f_{\mathrm{Mg}}(s) = \sum_{1s,2s,2p} f_{\mathrm{Mg},n}(s/\kappa_n) + q_1 f_{\mathrm{Mg},3s}(s/\kappa_{3s}),$$
$$f_{\mathrm{O}}(s) = f_{\mathrm{O},1s}(s) + q_2 f_{\mathrm{O},2s}(s/\kappa_{2s}) + 3q_2 f(s/\kappa_{2p}), \quad (1)$$

where $f_{A,n}$ is the scattering factor of orbital n for species A, κ_n is the relaxation parameter which controls the expansion/contraction of the orbital, and q_1 and q_2 are the occupancies of Mg $3s$ and O $2s$ orbitals, respectively. These were subsequently converted to electron scattering factors using the Mott formula. It is important to note that this is a parametrization of the electron density, so should not be overly interpreted with physical meaning. Such parametrizations are intrinsically nonconvex, so it is possible to have more than one functional form that gives the same density distribution.

We first fitted to the published bulk structure factors of MgO to determine a reference point. The deeply bound $1s$ core orbitals of both atoms are not significantly affected by crystal fields and, hence, their relaxation parameter was fixed at unity. The wave functions for the various orbitals in Eq. (1) were obtained from the self-consistent field calculations of Su and Coppens [11]. Gaussian bonding terms of variable width (B_n) and magnitude (q_n) (after Brill [12]) located between adjacent Mg-O atoms and O-O atoms were also used in some fits. The scattering from these "bonds" has the form $q_n \exp(-B_n s^2)$ in Fourier space. Table I lists the various fits to the published bulk structure factor measurements of MgO by Zuo *et al.* [3], Lawrence [13], and Sanger [14]. In addition to the aforementioned data sets, a mean inner potential of 12.52(24) V [3] was also used in the fitting process. Isotropic Debye-Waller factors were estimated at $B_{\mathrm{O}} = 0.335$ Å^2 and $B_{\mathrm{Mg}} = 0.308$ Å^2 in excellent agreement with previous studies [3,15]. Starting from the wave functions of the Mg atom and the O^- ion, various fits were attempted. The relaxations of the $2s$ and $2p$ orbitals of Mg show very similar trends and are almost identical in the fits with lower χ^2 values, namely, fits two and four. The relaxation of the valence orbitals of Mg and O are very sensitive to the occupancy of the Mg $3s$ orbital, which varies from 0.26 to 0.06. All four fits represent the same charge distribution, the difference being the way it is partitioned among the basis functions. The O valence orbitals are very diffuse, and to some extent extend to the Mg atoms. The relaxations listed in Table I are much higher than the previous fits of Zuo *et al.* [3] and Gillet *et al.* [15], and we believe this is due to the differences in the wave functions employed. The atomic scattering factors of Mg (in MgO) obtained from fit four are almost identical ($<1\%$) to those of Gillet *et al.* [15], while the omission of the charge in Mg-O and O-O bonds results in small differences ($\sim 2\%$) for O at low angles. It is well established that the oxidation state of Mg in bulk MgO is close to $+2$ and, hence, the fit that can be interpreted most physically is fit four. For all subsequent refinements of surface structure, the parameters of surface atoms were initialized from this fit.

The 2D symmetry of the surface structure is $p31m$, and anisotropic temperature factors consistent with the local symmetry of the various atomic sites were used. In addition to the in-plane positions of the second and third layer atoms, the relaxations and occupancies of the atoms in the top two layers were allowed to vary. The Mg atom in the third layer was constrained to be identical to the bulk Mg atom. In all refinements, the relaxations of the $2s$ and $2p$ orbitals of O were constrained to vary preserving the κ_{2s}/κ_{2p} ratio and the surface was also constrained to be charge neutral. Table II summarizes the results of the various fits to the surface data [16]. In all cases, the x, y positions refined to almost identical values which are shown in Table III, together with the z positions from density functional calculations discussed later. (Refinements with adsorbed surface species, for instance H atop the magnesium atom, resulted in much poorer fits.) The z

TABLE I. Results of model fitting of bulk charge density of MgO. B_3 and q_3 are parameters for the Mg-O bond, while B_4 and q_4 correspond to the O-O bond (see text for details).

	Mg			O								
	$(\kappa_n - 1)\%$	$(\kappa_n - 1)\%$	$(\kappa_n - 1)\%$	$(\kappa_n - 1)\%$	$(\kappa_n - 1)\%$							
Fit	$2s$	$2p$	$3s$	$2s$	$2p$	q_1	q_2	q_3	B_3	q_4	B_4	χ^2
1	13.7	−5.2	25.0	−16.4	1.8	0.26	1.93					1.42
2	18.9	−6.8	9.6	−10.4	0.4	0.19	1.90	0.04	6.70			1.20
3	12.1	−4.7	24.9	−14.2	1.0	0.20	1.93			0.01	1.74	1.38
4	18.2	−6.7	−25.0	−7.7	−0.7	0.06	1.90	0.04	7.35	0.02	2.76	1.11

TABLE II. Results of model fitting of the charge density of the MgO(111)-$\sqrt{3} \times \sqrt{3}R30°$ surface.

	Mg (layer 1)			O (layer 2)						
	$(\kappa_n - 1)\%$	$(\kappa_n - 1)\%$	$(\kappa_n - 1)\%$	$(\kappa_n - 1)\%$	$(\kappa_n - 1)\%$					
Fit	$2s$	$2p$	$3s$	$2s$	$2p$	q_1	q_2	q_3	B_3	χ^2
1	3.9	−18.0	5.0	−8.3	−1.5	0.43	1.87			1.49
2	−10.6	−15.0	5.0	−8.6	−1.8	0.38	1.88			1.51
3	18.2	−6.7	5.0	−4.3	2.8	0.43	1.87			1.57
4	2.8	−18.8	−18.0	−10.7	−4.0	0.00	1.89	0.08	2.32	1.50

positions were not used in the density fitting process. In the first three fits, the relaxation and occupancy of the $3s$ orbital of the top Mg atom are almost identical even though the $2s$ and $2p$ orbitals have very different relaxation parameters. All three cases have comparable χ^2 values of ~1.5, reflecting the similarities in the densities that they represent. (For reference, if the tabulated Mg^{2+} and O^{2-} [17] scattering factors were used, the χ^2 values were around 1.93. While the difference is not large, it is statistically significant.) The addition of a Mg-O bond term, similar to the one in bulk fitting, results in the siphoning of the electrons from the valence orbitals of Mg to those of O and the bond. If we simply take the orbital occupancies as a measure of the oxidation states, we find for the top Mg and second layer O atoms $+(1.65 \pm 0.1)e$ and $-(1.52 \pm 0.1)e$, respectively, relative to bulk values of $+1.94e$ and $-1.72e$ (ignoring the charge located between the Mg and O atoms, q_3 in Tables I and II). In some respects, these numbers are misleading, and a better physical interpretation is to look at the two-dimensional projected valence shell deformation density shown in Fig. 2. Although there is more nominal charge in the Mg $3s$ orbital, the valence orbitals are expanded with respect to the bulk atom which results in a negative difference in the region very close to the core. The O atom is contracted with respect to the bulk, consistent with less charge in its valence shell, which is reflected in the negative contours around the O sites. The electron hole in the second layer is quite diffuse, spread over a radius of ~1 Å centered on the O sites, as evident in Fig. 3. An interesting feature that is evident in the deformation map is the region of increased density along the Mg-O direction indicative of a weak covalent bond, manifested as the truncation of the negative lobe around the O sites.

The MgO surface structure was separately optimized using a density functional theory (DFT) surface slab model of 13 layers (35 atoms). This provides for both an independent confirmation of the experimentally determined x, y (or in-plane) atomic positions as well as the missing z atomic positions. All calculations were performed using the *ab initio* total energy program VASP [18,19]. The generalized gradient approximation [20], ultrasoft pseudopotentials [21], and a plane-wave basis set with a 400 eV cutoff were used. Brillouin zone integrations were performed on a $4 \times 4 \times 1$-Monkhorst-Pack grid [22].

To estimate the charge transfer independent of the experimental fits, partial atomic charges were also computed using the empirical bond-valence model [23] which requires only the atomic positions (here the DFT optimized structure) as input. The results are included in Table III, and for the top atoms correlate very well with what was found in the experimental fits. The changes in bond lengths lower down in the structure also yield some apparent bond-valence changes. These changes were not observed in the experimental data and are presumably artifacts of the empirical method.

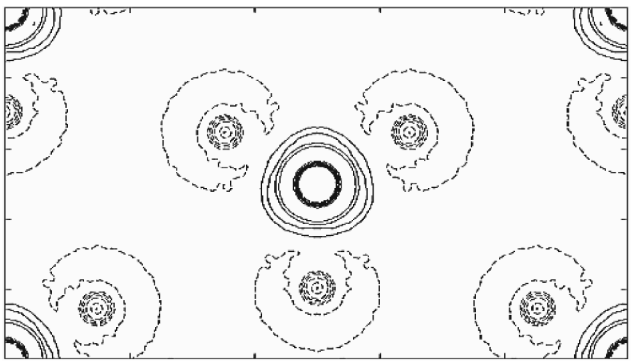

FIG. 2. Deformation charge density map projected onto the (111) plane. The contour interval is $1.5 \times 10^{-4} e^-/\text{Å}^2$.

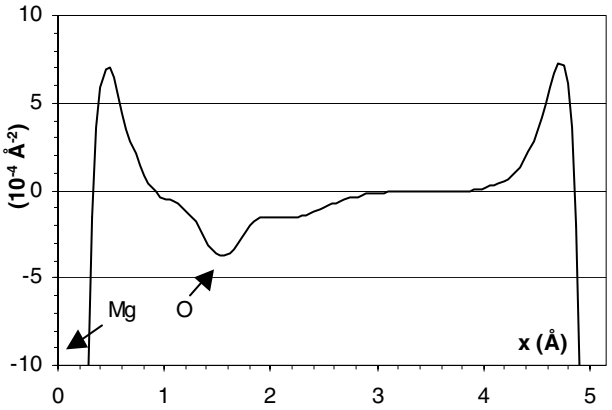

FIG. 3. Line plot of the deformation density along a side of the unit cell (i.e., along the diagonal in Fig. 2).

TABLE III. Coordinates and oxidation states of the various atoms in MgO(111)-$\sqrt{3} \times \sqrt{3}R30°$ surface. $a = b = 5.15$ Å, $c = 7.30$ Å, $\alpha = 90°$, $\beta = 90°$, and $\gamma = 120°$.

		Experiment			DFT			
Layer	Atom	x	y	$q(e)$	x	y	z	$q(e)$
1	Mg	0	0	+1.65	0	0	0.627	+1.69
2	O	0.294	0	−1.52	0.321	0	0.499	−1.67
3	Mg	0.662	0	+1.94	0.652	0	0.344	+2.00
4	O	0	0	−1.96	0	0	0.168	−1.77
4	O	1/3	2/3	−1.96	1/3	2/3	0.168	−1.94
4	O	2/3	1/3	−1.96	2/3	1/3	0.168	−1.94
5	Mg	1/3	0	+1.94	0.332	0	0	+1.95

Unfortunately, there is no unambiguous method of extracting either a deformation map relative to the bulk or the degree of charge transfer from this type of DFT code; the O^{2-} reference state required for deformation maps vs free ions is unstable as an isolated ion. The small changes that show when an appropriate bulk reference state is used with the experimental data would be masked if O^{-} or O reference states were used. The experimentally fitted bulk density is not a viable reference either as the densities near the core are not correctly represented by pseudopotential methods [24].

If one formally considers the surface as composed of Mg^{2+} and O^{2-} building blocks, an additional electron hole per surface unit is required to make the reconstruction charge neutral. Our results indicate that this hole is located in the second layer O atoms. There is also an increased covalency at the surface (about twice that of the bulk) which is manifested as an increased density between the Mg and O atoms and a nominal transfer of electron density from the orbitals of O to those of Mg (for reference, increased covalency would lead to less positive and less negative charge on Mg and O, respectively; the hole would make Mg more positive and the O less negative). From a simplistic point charge model, the present stacking sequence, Mg_1–$(O_3 + h)$–Mg_3, intrinsically has a very small net dipole moment. This is further reduced by an inward relaxation (by 23%) of the first layer Mg atom seen in the z positions from the DFT calculations. The observed orbital relaxations, namely, the contraction of the O^{2-} ion and the expansion of the Mg^{2+} ion, are also consistent with the observations of charge transfer from O^{2-} to Mg^{2+}. Note that the charge localization and orbital relaxations were independent variables in the refinements, so the fact that they change in directions which make physical sense is encouraging.

This work was supported by the National Science Foundation by Grant No. DMR-007-5834.

*Author to whom correspondence may be addressed.
Current address: 2220 Campus Dr., Cook Hall No. 2036, Evanston, IL 60208-3108, USA.
Electronic address: arun@risc4.numis.nwu.edu

[1] C. Noguera, J. Phys. Condens. Matter **12**, R367 (2000).
[2] J. Cowley, Acta Crystallogr. **6**, 516 (1953).
[3] J. M. Zuo, M. O'Keeffe, P. Rez, and J. C. H. Spence, Phys. Rev. Lett. **78**, 4777 (1997).
[4] J. M. Zuo, M. Kim, M. O. O'Keeffe, and J. C. H. Spence, Nature (London) **401**, 49 (1999).
[5] L. D. Marks, N. Erdman, and A. Subramanian, J. Phys. Condens. Matter **13**, 10 677 (2001).
[6] D. Wolf, Phys. Rev. Lett. **68**, 3315 (1992).
[7] M. Gajdardziska-Josifovska, P. A. Crozier, and J. M. Cowley, Surf. Sci. Lett. **248**, L259 (1991).
[8] R. Plass *et al.*, Phys. Rev. Lett. **81**, 4891 (1998).
[9] B. Dawson, Acta Crystallogr. Sect. A **25**, 12 (1969).
[10] R. F. Stewart, J. Chem. Phys. **58**, 1668 (1973).
[11] Z. Su and P. Coppens, Acta Crystallogr. Sect. A **54**, 646 (1998).
[12] R. Brill, Acta Crystallogr. **13**, 275 (1960).
[13] J. L. Lawrence, Acta Crystallogr. Sect. A **29**, 94 (1973).
[14] P. L. Sanger, Acta Crystallogr. Sect. A **25**, 694 (1969).
[15] J.-M. Gillet and P. Cortona, Phys. Rev. B **60**, 8569 (1999).
[16] See EPAPS Document No. E-PRLTAO-91-044349 for the table fittings to the experimental data from the reconstructed MgO(111) surface. A direct link to this document may be found in the online article's HTML reference section. The document may also be reached via the EPAPS homepage (http://www.aip.org/pubservs/epaps.html) or from ftp.aip.org in the directory /epaps/. See the EPAPS homepage for more information.
[17] D. Rez, P. Rez, and I. Grant, Acta Crystallogr. Sect. A **50**, 481 (1994).
[18] G. Kresse and J. Hafner, Phys. Rev. B **47**, 558 (1993); **49**, 14 251 (1994).
[19] G. Kresse and J. Furthmuller, Comput. Mater. Sci. **6**, 15 (1996); Phys. Rev. B **54**, 11 169 (1996).
[20] J. P. Perdew *et al.*, Phys. Rev. B **46**, 6671 (1992).
[21] G. Kresse and J. Hafner, J. Phys. Condens. Matter **6**, 8245 (1994).
[22] H. J. Monkhorst and J. D. Pack, Phys. Rev. B **13**, 5188 (1976).
[23] N. E. Brese and M. O'Keeffe, Acta Crystallogr. Sect. B **47**, 192 (1991).
[24] J. R. Trail and D. M. Bird, Phys. Rev. B **60**, 7875 (1999).